Present-day crustal deformation derived from continuous GPS array: a study case of Japan

Gamal El-Fiky [a], Ashraf Mousa [a], Mostafa Rabah [a] and Hassan El-Ghazoly [b]

[a] *National Research Institute of Astronomy and Geophysics, Helwan, Cairo, Egypt*

[b] *Transportation Eng. Dept., Faculty of Eng., Alexandria University, Alexandria , Egypt*

Least squares prediction using two empirically deduced local covariance functions was applied to estimate the crustal strains in the Japanese islands. Data from the nation-wide GPS continuous tracking network that has been operated by the Geographical Survey Institute of Japan since April 1996 were used. We first extracted site coordinate from daily SINEX files for the period from April 1st, 1996 to August 31st, 1999, and estimated average site velocity by linear regression. Estimated velocities converted into a kinematic reference frame to discuss the crustal deformation relative to the stable interior of the Eurasian plate. To segregate the signal and noise in the velocity vectors by least-squares prediction technique, we first derived two covariance functions of the velocity vectors, one for the E-W component and the other for N-S component, with a Gaussian form. Estimated signals (displacement vectors) were then differentiated in space to calculate principal components of strains. Obtained strains; dilatations, maximum shear strains and principal axes of strains are clearly portray tectonic environments of the Japanese islands. Directions of the maximum compressive strains estimated in the present are in a good agreement with those of long-term strains rate estimated from seismological and geological data. On the other hand, the shear stresses at surface of the Japanese islands have been estimated, based on elastic theory. The obtained stresses by surface observation were compared with the shear wave splitting data that show directions of maximum compression of the upper crust. Results show a general correlation with GPS stresses, suggesting that the stresses observed at the surface may represent upper crustal stresses, though some exceptional areas exist such as Shikoku and western part of Kyushu.

تم في هذا البحث تطبيق نظرية أقل مجموع للتبؤ باستخدام دالة المتغيرات المتبادلة وذلك لتقدير مقدار انفعال القشرة في الجزر اليابانية وقد تم تطبيق هذه النظرية على الجزر اليابانية وذلك لغزارة المعلومات التى تم الحصول عليها من المحطات الأرضية وذلك من إبريل ١٩٩٦ وحتى ٣١ أغسطس ١٩٩٩. وقد تم تقدير متوسط سرعة الموقع وذلك لشرح تشوهات القشرة الأرضية بالنسبة إلى الثبات الداخلي للوح الأوروأسيوى (Eurasian plate). حيث تم الفصل بين الإشارة والضوضاء فى متجه السرعة بواسطة نظرية أقل مجموع للتنبوء كما تم في هذا البحث تقدير مقدار إجهاد القص عند السطح للجزر اليابانية وذلك بواسطة نظرية المرونة وقد انتهى البحث إلى أن أقصى إجهاد قص يظهر تطابق جيد مع نشاط القشرة الحالي كذلك فإن المحاور الرئيسية للانفعال أظهرت أن الجزر اليابانية تقع تحت تأثير ألواح المحيط. كما توصل البحث إلى أن اتجاه أقصى انفعال ضغط تم تقديره حالياً يكون متوافق توافقاً جيداً مع البيانات الزلزالية والجيولوجية كذلك أظهر البحث أن معدل الانفعال الحادث فى أرصاد (GPS) أعلى بمقدار عشرة وحدات عن انفعال المدى الطويل المقدر من البيانات الزلزالية والجيولوجية. وفي النهاية فقد تم تقدير اجهادات القص عند السطح للجزر اليابانية بواسطة نظرية المرونة وقد قورنت مع الإجهادات من أرصاد (GPS) مع بيانات القص للموجات والتي تظهر أقصى انضغاط للقشرة السطحية وقد أظهرت النتائج توافق عام مع نتائج اجهادات (GPS).

Keywords: Crustal strains, Shear stresses, GPS, Least-squares prediction LSP, Elastic theory

1. Introduction

Monitoring the crustal strain perturbations is a key to understand the physical process in the crust as well as to forecast the crustal activity. Dense arrays of continuous GPS tracking networks provide us with one of the ideal tool for monitoring crustal strain. In Japan, the Geographical Survey Institute (GSI) started to establish the dense GPS array of continuous tracking network in the Kanto-Tokai region in 1992 and has further expanded it to cover the entire nation. The GSI has been operating 610 sites, for continuous monitoring of the daily site coordinates since April 1996. The number of sites went up to

1000 by 1997, with average site intervals of about 20 km [1-3]. The array is now considered as one of the most fundamental infrastructures for monitoring crustal activity in Japan. Details of the operation and analysis of this GPS array are described in [1, 2].

There are a variety of methods to delineate crustal strains [4-10]. However, all of these studies use a discrete approach where the area within a particular triangle or block is assumed to have uniform infinitesimal strains. The reality is such that the land deforms rather continuously except where/when a fault displaces the land surface. Thus, a more appropriate technique to represent crustal strains in a continuous manner may have to be used. Some researchers have used algebraic polynomials of specified degree to describe crustal strains [11-13]. Also, recently, [14] used an assumed distances decaying constant to relate the observed displacement rate with the strain rate tensor. However, such purely mathematical approach could sometimes yield spurious results. We would rather like to use some physical information included in data itself. One of relevant techniques is the least squares prediction whereby tectonic signal in the data is extracted by the statistical analysis of data themselves.

Tectonic settings in and around the Japanese islands are not simple but have a wide variety of features because the islands are located at the complex plate boundaries configured by four major plates fig. 1. Estimated displacement field of the Japanese islands from the above GPS array [15] indicated a prominent westward motion of the northeastern part of Japan and a northwest-ward movement of the southwestern part of Japan. This is clearly due to the effects of the subducting oceanic plates under the Japanese islands. In the present study, we try to delineate the crustal strains of the Japanese islands, using data for about three and half years from the above GPS array fig. 1. For this purpose, we first extracted site coordinate from daily SINEX files for the period from April 1st, 1996 to August 31st, 1999, and estimated average site velocity by linear regression. Estimated velocities are converted into a kinematic reference frame [16] to discuss the crustal deformation relative to the stable interior of the Eurasian plate. We, then, applied the Least-squares prediction technique for strain field analysis. Obtained GPS strains rate was compared with long-term strains rate estimated from seismological and geological data. Also, the shear stresses rate at surface of the Japanese islands was estimated, based on elastic theory. The stresses obtained by surface observation were compared with the shear wave splitting data that show directions of maximum compression of the upper crust. Finally, results of stains and stresses are discussed with reference to the tectonic of the Japanese islands.

2. Least-squares prediction technique

To delineate crustal strains in the Japanese islands, we applied the Least-Squares Prediction (LSP) method that has been developed by [17] for the reduction of gravity data, and was applied to the crustal deformation data by [18]. The method is a corollary of the Least Squares Collocation technique (LSC), and was discussed in briefly in previous papers [18, 19]. In the present paper, the detail of the method is explained and the results of its application are shown for the study distribution of horizontal strains in the Japanese islands. At same time, emphasis will be laid on the effects of the covariance functions on the estimated crustal strains.

In the LSC, the crustal deformation data l is assumed to be composed of systematic errors, tectonic signal and noise so that it is expressed by the following observation equation;

$$l = Ax + t + n . \qquad (1)$$

Where A is a known coefficient matrix, x is the vector of unknown parameters, t is the signal vector at the observation points, and n is the vector of the noise that represents the measuring error. For example, a linear trend in gravity data or systematic error in levelling are considered in x. Signal t and noise n are assumed to be unbiased so that E(t)=E(n)=0, where E denotes statistical expectation.

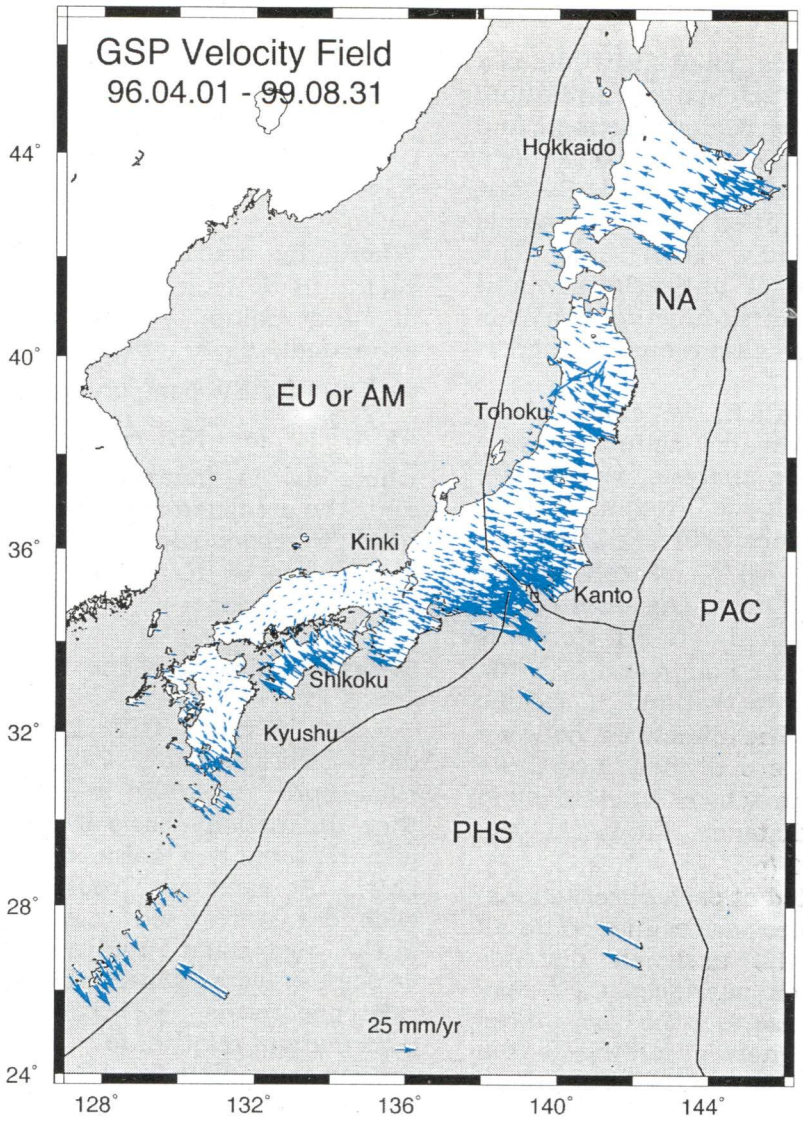

Fig. 1. Yearly averaged velocity vectors obtained from the continuous GPS observation network in the Japanese islands for the period April 1996 to August 1999. EU or AM (Eurasian or Amurian) plate, NA (North American) plate, PHS (Philippine Sea) plate and PAC (Pacific) plate.

In the daily solution of GPS dense arrays, systematic baseline biases are removed in the daily baseline analysis, so that the resultant coordinates may be assumed to be systematic errors-free. Suppose that such systematic part Ax is removed in advance from data. Then we consider only the non-parametric part, so that eq. (1) may be written in the following form:

$$l = t + n. \qquad (2)$$

This equation simply means that the data l is composed of tectonic signal and random noise. Here, the signal is the tectonic deformation that arises from inside and outside of the region. Noise is erroneous fluctuations that are inherent in each of the GPS sites. Monument instability, antenna multipath, underground water flow, and so on are causes for such noise [20]. This noise may have to be removed to obtain crustal deformation of tectonic origin. Thus, the problem is to extract the signals at any location from/by some filtering technique, considering that the noise n is limited to only the site or adjacent local regions and tectonic signals may have rather wider correlation in nature [19]. Thus, a hypothesis to separate these components is given in which the signal has spatial correlation whereas the noise does

not. Variance-covariance analysis of data is a good measure to find such spatial correlation. If we assume that the field is isotropic and homogeneous, the covariance of data is only a function of site distance "d" [18]. Such a function may be fitted by a simple mathematical function. Then we can reconstruct the signal at any arbitrary grid points S using thus fitted function, which is called the Empirical Covariance Function (ECF) [19].

From GPS observation, we obtain three dimensional site coordinates estimated every day. By linear regression analysis, we estimate yearly velocities at each site. From such data, we calculate the variance $C_l(0) = (\sum l_i l_i)/N$ and covariance $C_l(d_p) = (\sum l_i l_j)/N_p$ of the data for each component, after removing averages of vectors to make non-biased data set. Here N is the total number of data points and N_p is the number of data points within a specific distance interval d_p. The distances between two data points d are divided into finite discrete intervals P, in which N_p $(1 \le p \le P)$ data pairs whose distance drops in the interval $(p-1)\delta < d_p \le (p)\delta$, $(p = 1, 2, 3, ...P)$. Variances are estimated at each observational site, whereas covariances are estimated for all site pairs within the assigned distance interval. Thus obtained variances $C_l(0)$ may include signal and noise, but the covariances $C_l(d_q)$ include only signals according to the above hypothesis. The plot of the covariances with respect to distance would be a curve that naturally diminishes with distance. One simple mathematical function to express such plots would be a Gaussian function in the following form, $C_l(d_i) = C_t(0) \exp(-k^2 d_i^2)$, which we choose here as the empirical covariance function (ECF). Two parameters $C_t(0)$ and k are fitted from a covariance plot of the data. $C_t(0)$ is the expected variance at the sites and $C_r(0) = C_l(0) - C_t(0)$ is considered the noise component at the site. Parameter k is an indication of how far the correlation distance reached, which has the dimension of inverse distance. Finally, the defined Gaussian function $C_l(d)$ is used to compose C_l, and C_{st}, the covariance matrix of observation, and the covariance matrix between the data points and other grid points where signals are to be estimated, respectively. Once such ECF is obtained, we can estimate signal S at any arbitrary location by the following equation [18];

$$S = C_{st} C_l^{-1} /. \qquad (3)$$

Where the matrix C_{st} is composed of elements $c_{st}(1 \le t \le N, 1 \le s \le m$, where m is the number of grid points whose signals are to be estimated); c_{st} is given by $c_{st} = C_{ut}(0) \exp(-k_u^2 d_{st}^2)$ for EW component and $c_{st} = C_{vt}(0) \exp(-k_v^2 d_{st}^2)$ for NS component, respectively, where d_{st} is distance between the data site and the predicted site. The above formula was used to reconstruct velocity vectors (signal) at grid points of 10 km × 10 km mesh covering the study region.

3. Crustal strains of the Japanese islands

Data of GSI's GPS array are provided as daily SINEX format. We used daily GPS data from April 1st, 1996 to August 31st, 1999, so that the period spans about 3.3 years, which give reasonably reliable displacement vectors [2,21]. At each site, coordinate differences of each day were used to estimate velocities by linear regression analysis. Then, estimated velocities were converted into a kinematic reference frame by [16] to discuss the crustal deformation relative to the stable interior of the Eurasian plate fig. 1.

Since the displacement vectors fig. 1 include effects of the volcanic activity of Iwata area (northern part of Tohoku) of September 1998, therefore, we did not use vectors of this area in the estimation of covariance functions. The number of data point used was 911 out of 917. After this, systematic bias is removed from all site velocities by subtracting the average of velocities. Then, we applied the LSP as described above to each of the vector components (East-West and North-South) independently. ECF for each of the components are fitted to the data. After that, ECFs are used to reconstruct displacement vectors (signal) at gridded points (10 km x 10 km) mesh covering the Japanese islands.

We used δ = 30 km as the discrete interval to estimate covariances, $C_l(d_q)$. The obtained variance-covariance plot and fitted ECFs are

shown in figs 2-a and 2-b. The east-west component where C_{lu} is the variance-covariance of velocity vectors and the north-south component where C_{lv} is the variance-covariance for this component are shown in fig. 2-a and fig 2-b, respectively. Then estimated velocities at grid points are differentiated in space to obtain crustal strains in this data period. Figs 3, 4, and 5 are the estimated dilatational strains, maximum shear strains, and principal axes of strains, respectively.

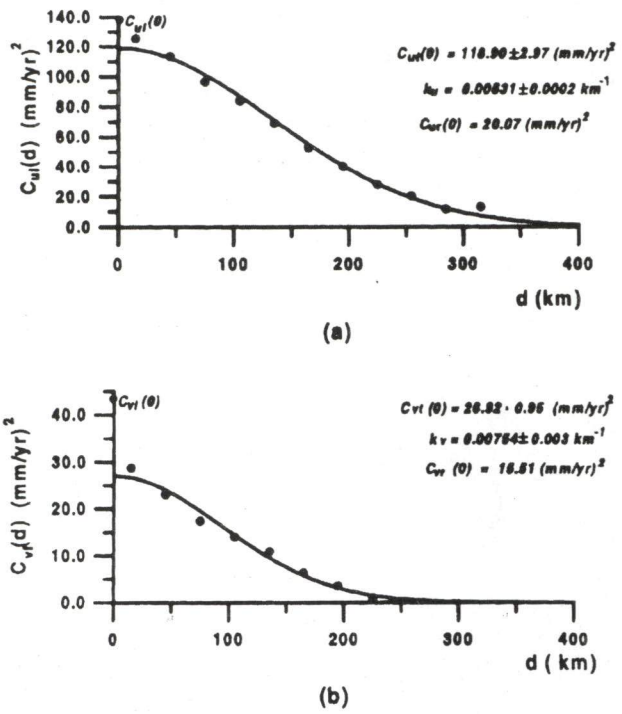

Fig. 2. Variance- covariance of displacement vectors for discrete baseline distances and fitted empirical covariance functions; (a) EW component, and (b) NS component, respectively. Estimated parameters ($C_{ut}(0)$, $C_{ur}(0)$ and k_u) for EW component and ($C_{vt}(0)$, $C_{vn}(0)$ and k_v) for NS component are shown in the figure.

The obtained covariance functions figs 2-a and 2-b approach zero at distances of about 300 km and 250 km for EW component and for NS component, respectively. These correlation distances are about half of that of Eastern Mediterranean region [22]. This difference in correlation distances may reflect different tectonic settings between the Eastern Mediterranean and the Japanese islands or this might indicate that the characteristic wave-length of crustal deformations (crustal blocks) are a little less fragmented in the Eastern Mediterranean region compared with to Japanese islands.

4. Characteristics of ECF

Least-squares prediction depends mainly on the choice of the covariance functions and the determination of its parameters. In this section, the effects of changing parameters ($C_t(0)$, $C_r(0)$, and k) of the covariance functions on the estimated horizontal strains are studied. Although it may be necessary to introduce a statistical approach to investigate such effects, we limit the discussion simply by showing some examples.

First of all, we examined the effect of the change in the number of GPS sites. We have tried several cases reducing the number of sites; 5%, 10%, 15%, and 25%. One example is shown in fig 6 where 700 sites out of 917 sites (about 25% reduction) were used. Reproduced pattern of maximum shear of strains rate is approximately the same as fig. 4. Thus we could conclude that the reduction of the number GPS sites up to 25% is tolerable for predicting the rate of crustal strains in the Japanese islands. Increasing the number of observed signals might give a more detailed pattern for the predicted crustal strain.

Next, we examined the effect of changing parameters of the Gaussian function that is used in this study. When the observation error is not considered, i.e., $C_r(0)=0$, the least squares prediction becomes a pure least squares interpolation. In this case, estimated signal is controlled only by parameter k [18]. On the other hand, when the observation error is considered, i.e., $C_r(0)\neq 0$, both k and $C_t(0)$ have considerable effects in estimating the signal. In this case, the variance of signal $C_t(0)$ and the variance of noise $C_r(0)$ can be treated as only one independent parameter, because there is a relation between $C_t(0)$ and $C_r(0)$ such that the small change (ε) of $C_t(0)$, from $C_t(0)$ to $C_t(0) + \varepsilon$ is equivalent to the change of $C_r(0)$ to

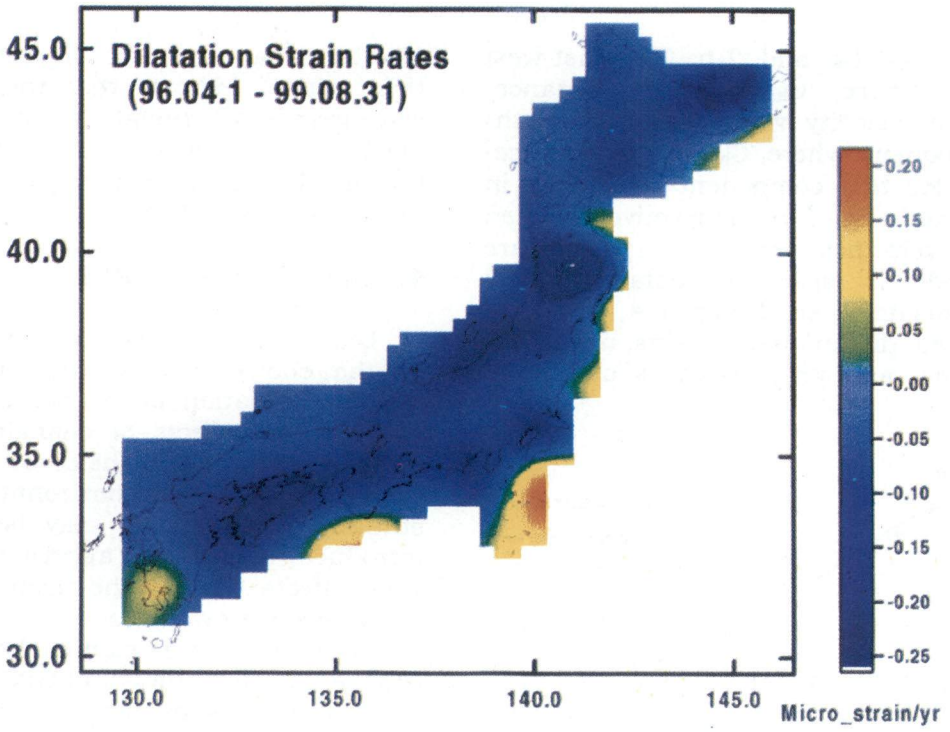

Fig. 3. The areal dilatation of the Japanese islands as estimated by the LSP technique for the period from April 1st, 1996 to August 31st, 1999. Unit is Micro strain/yr.

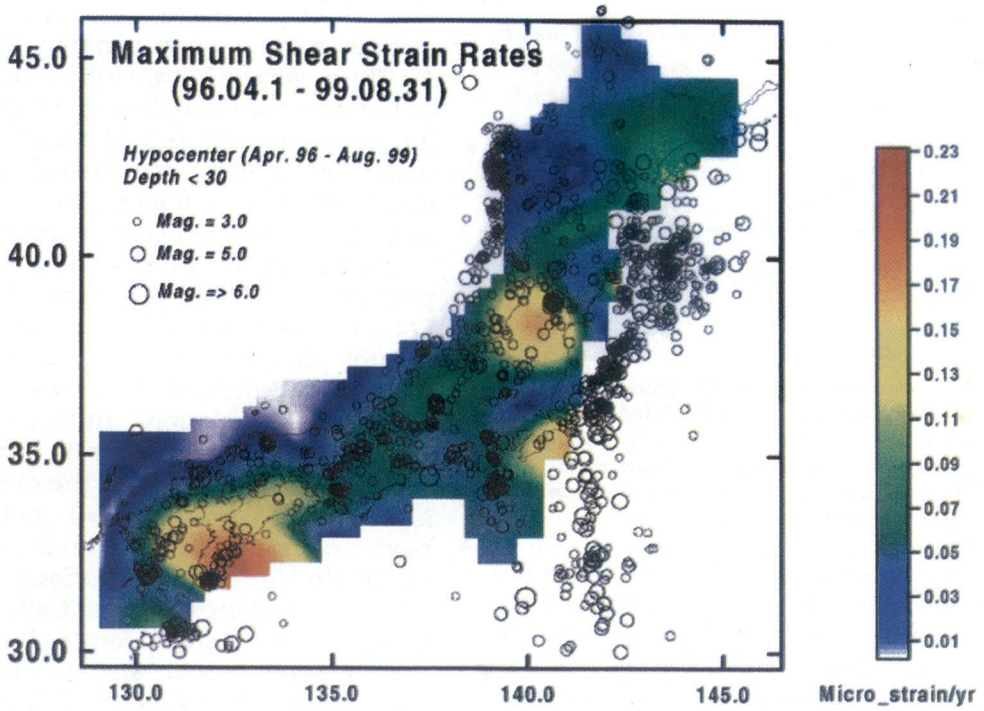

Fig. 4. Distribution of the maximum shear strain rates in the Japanese islands as estimated by LSP for the period from April 1st, 1996 to August 31st, 1999. Unit is Micro strain/yr.

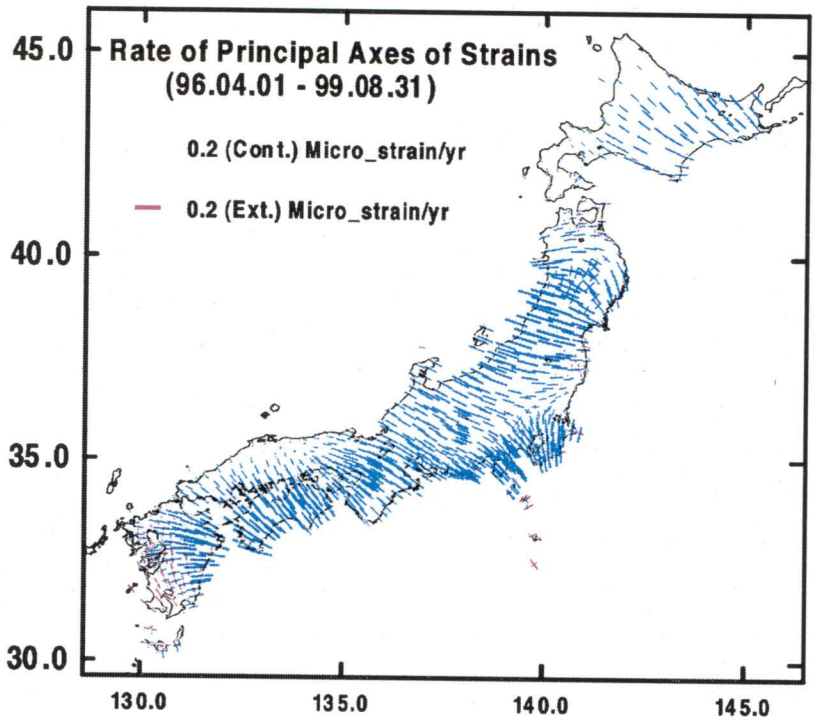

Fig. 5. Magnitude and orientation of principal strains axis in the Japanese islands as estimated by LSP for the period from April 1st, 1996 to August 31st, 1999. Unit is Micro strain/yr.

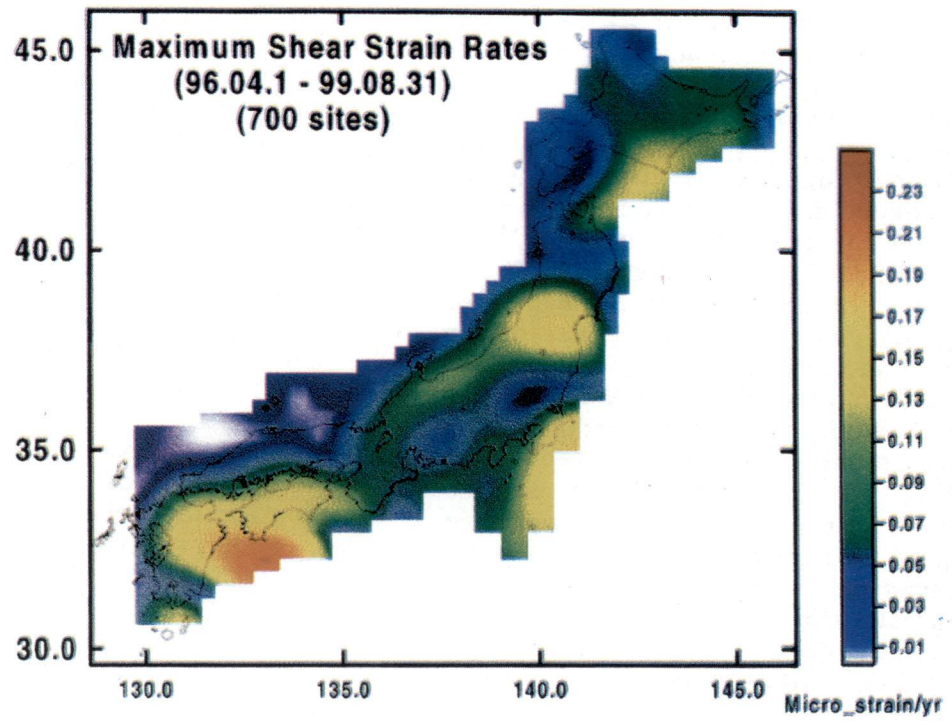

Fig. 6. Distribution of the maximum shear strain rates in the Japanese islands as estimated from observed 700 GPS sites by LSP method. Unit is Micro strain/yr.

$C_r(0)C_t(0) / \{C_t(0) + \varepsilon\}$ [18]. To see the effect of changing these parameters, we changed the variance of signals by reducing $C_t(0)$ to $75\% \times C_t(0)$ in E-W and N-S components and keeping the variance of noise $C_r(0)$ constant. The results are shown in fig. 7. It can be seen that the pattern of maximum shear of strains in this figure are almost the same as in fig. 4. This suggests that the change in $C_t(0)$ by 25% does not affect the predicted strains. As mentioned above, the reduction of $C_t(0)$ to $0.75 \times C_t(0)$ is equivalent to the increase of $C_r(0)$ to $1.33 \times C_r(0)$ and the change in the ratio $C_r(0)/C_t(0)$ is small, 15% at most, so that it does not have much influence on the predicted strain rates.

Then, effect of changing the parameter k is investigated. The inverse of k implies the areal correlation distance between two horizontal displacements of the same component. When k is large, the correlation distance will be short, and vice versa. We have tried several cases of increasing and decreasing of k; 5%, 10%, 20%, and 35%. We found that predicted strains far way from observed sites are much influenced by the parameter k. Generally, we can say a small change in k up to 20% does not change the pattern of the crustal strains, but the pattern becomes smoother when k is smaller.

Finally, we investigated the effect of the using the parameters ($C_t(0)$, $C_r(0)$, and k) of the covariance function for the entire Japan on the estimated distribution of crustal strains of some local areas. Here we used the Hokkaido and Kyushu islands as two examples for the locale areas. We estimated the empirical covariance functions of the Hokkaido and Kyushu islands using the present data interval for each area. Figs 8-a and 8-b show the above estimated functions and fitted parameters for the two areas. Considering the above discussion for the changing in the parameters of covariance function, we can say the correlation distance, which represents by the parameter k will be the most affective parameter in the local covariance functions. Using these covariance functions we recalculated the strain components in the two areas. Fig. 9-a and 9-b shows the principal axes in both of them as an example for the strains components. It is readily seen that the estimated principal axes of stains in these figures are almost the same as that in the Hokkaido and Kyushu areas in fig. 5, but some differences exist. The differences may be attributed to two reasons. The first is the effect of the ratio $C_r(0)/C_t(0)$ in E-W and N-S components. Since the velocity field of the Japanese islands indicate a prominent westward motion in NE Japan and NW movement of SW Japan, the effect of the ratio $C_r(0)/C_t(0)$ in E-W has a more influence compared with the other component. However, this ratio has not a remarkable changed figs.. 8-a and 8-b. The second is that, the shorter correlation distance of the local covariance functions. In fig. 5 in which covariance function was applied for the entire Japanese island, the correlation distance was about 300 km. So, the short wave length of crustal deformations in the Japanese island might be removed to some extent through the filtering effects of parameters $C_{ur}(0)$ and $C_{vr}(0)$ in the covariance functions. On the other hand, in fig. 9 in which local covariances were used for the Hokkaido and Kyushu area, the correlation distances is 180 km and 150 km, respectively. Therefore, a more detailed pattern for the predicted of the horizontal strain was seen along the pacific coast in Hokkaido and most southern part of Kyushu areas fig 8-a and 8-b. Even though least squares prediction predicts the crustal strains based on all the known data, the strain components are much influenced by the closest data sites. The regional and local covariance functions are coincided in the range from 0 to 180 km for Hokkaido and 0 to 180 km for Kyushu that have much influenced on the strain components. The covariance function in the longer distances has a small influenced as see in the fig. 9. After that, we have tested several cases of changing in correlation distances of the above covariance functions on the estimated strains in the local areas. Finally we can say using a regional covariance functions in a regional area (e.g., Japanese island) does not change the pattern of the crustal strain distribution in a specific local area within this regional area, but the short deformation features might it be possible for seeing when local covariance is used.

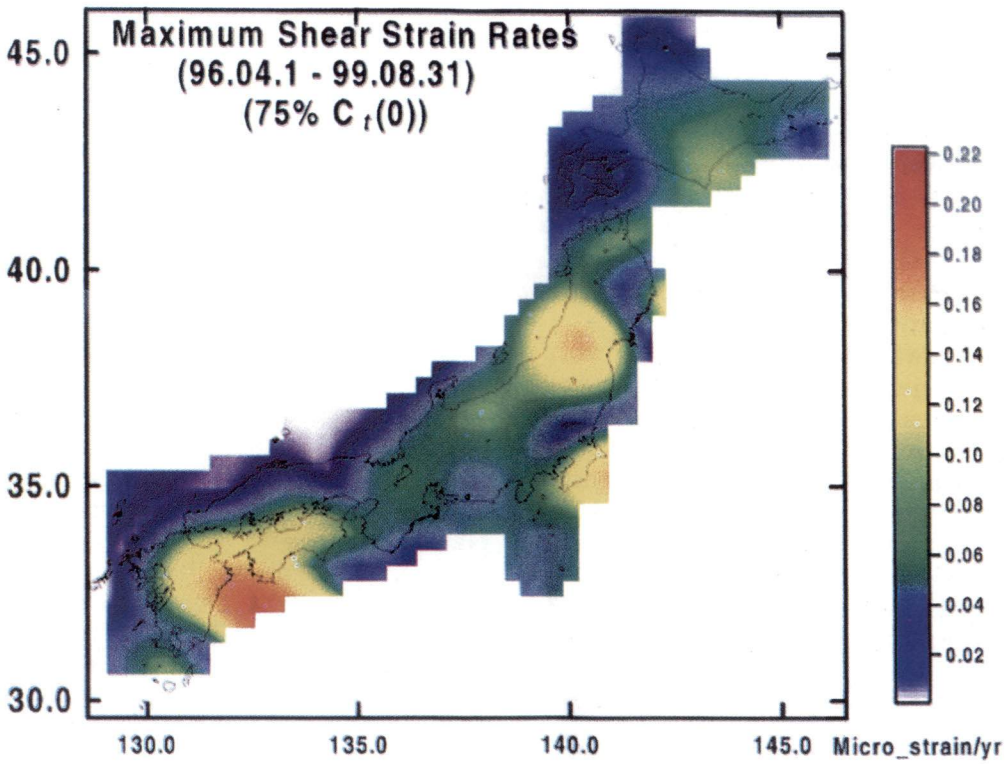

Fig. 7. Distribution of the maximum shear strain rates in the Japanese islands as estimated by LSP method. The variance of the signal of the covariance functions in E-W and N-S components was decreased by 25%. Unit is Micro strain/yr.

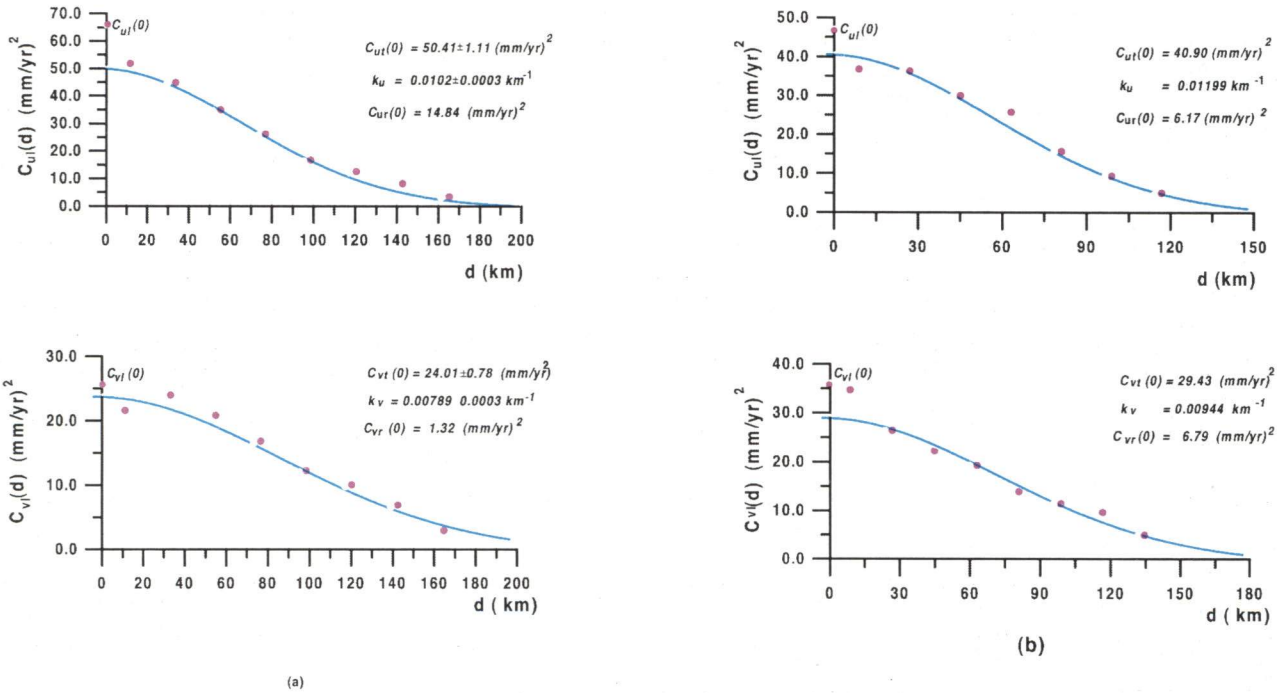

Fig. 8. Variance- covariance of displacement vectors for discrete baseline distances and fitted empirical covariance functions; (a) Hokkaido island, and (b) Kyushu island, respectively. Estimated parameters ($C_{ut}(0)$, $C_{ur}(0)$ and k_u) for EW component (the upper figure) and ($C_{vt}(0)$, $C_{vn}(0)$ and k_v) for NS component (the lower figure) of each area are shown in the figure.

5. Discussion

Figs 3 to 5 show estimated dilatation strains, Maximum shear of stains and principal axes of strain in the data period, respectively. These figures, though estimated from relatively a short interval of data, may well portray characteristics of the tectonic strains in the Japanese islands.

Firstly, the dilatational strain rates shown in fig. 3 indicate that the Japanese islands are under the compressional strain regime. This may be due to the subducting oceanic plates from east, Pacific plate, and southeast, Philippine Sea plate, fig. 1 and might be also due to the eastward extraction of China continental block by the collision of India toward north [21]. Large (>0.2 Microstrain/yr) compressional strain is found in the eastern Hokkaido, central Tohoku, the Japan Sea coast of Tohoku, and all over Shikoku district. The large compressional strain along the Japan Sea coast is an important issue derived from the present GPS data. This may support the incipient subduction and the new plate boundary in this region as suggested by several researchers [23, 24]. On the other hand, widespread compressional strain is in fig. 3 somewhat different from data obtained by conventional surveys. [25] analysed the strains in the Japanese islands by the triangulation data for the last 100 years and showed that the dilatational strain is positive in most of Tokoku and Kyushu districts, which significantly differ from the present results. The present study shows that only the southern parts of Kyushu are dilating positively. Discrepancy in the Tohoku district may have to be examined carefully because many interplate earthquakes have occurred in the past 100 years and affected strains in the area. Although none of the large interplate earthquakes have occurred in the Tohoku area in the studied period, significant postseismic deformation occurred especially in the northern part of the area after the Sanriku earthquake of 1994 (M 7.5) [26, 27].

Maximum shear strain rates fig. 4 show some patches of high values of strain. They are over; the southeastern part of Hokkaido, southern Tohoku, southern Kanto, Shikoku, and southeastern Kyushu. These areas coincide with seismically active regions. To compare the maximum shear strains with seismicity data, epicentres of shallow earthquakes of depth less than 30 km are plotted in fig. 4. Southeastern Hokkaido is an area where a couple of large offshore earthquakes occurred; 1993 Kushiro earthquake and 1994 Hokkaido-Toho-oki earthquake [28]. A wide area in the southern part of Tohoku has high maximum shear. At the northern edge of this area, the largest magnitude of inland earthquake occurred in the studied period was the Narugo earthquake (M 5.9) of August 11th, 1996. South Kanto is the region where the Philippine Sea plate converges to the North American (or Okhotsk) plate seismic and volcanic activities are very high. On the other hand, the strain rates in this region might be partly attributed to the silent earthquake off Boso peninsula in May 1996, which followed by a number of small earthquakes [29]. High maximum shear in the Shikoku region may be due to the oblique subduction along the Nankai trough [30], eastward motion of the Amurain plate [31], and/or the N-S oriented extension in Kyushu associated with expansion of the Okinawa trough [32]. Finally, northeastern part of Kyushu is most prominent in this figure. This may be due to coseismic and postseismic effect of Hyuganada earthquakes of October 19th (M 6.6) and December 3rd (M 6.3), 1996 [33]. The slow thrust slip event of May 1997 following the above Hyuganada earthquakes, also, might have contributed to this high strain rate in this area as suggested by [34].

Fig. 5 shows magnitudes and directions of principal strain axes. Even though the east-west compressional stain is predominant in the Kyushu island, a north-south extension is also evident there. [32], using the conventional surveys, hypothesized that Kyushu area is under the extensional force due to the rifting at the Beppu-Shimabara Graben in the northern Kyushu. The present GPS data is somehow consistent with the conventional strain data, however, the stains pattern seems different. Apart of this, NW-SE compression is predominant in the southwestern Japan. This may be due to the compressional force acting at the convergent plate between the Philippine Sea plate and the continental plate Tada [35]. The northeastern Japan exhibits east-west compressional strains due to the Pacific plate

converging toward west, whose directions are consistent with the result obtained by the old triangulation data by [36, 19], but the magnitudes are about twice larger relative to their result.

5.1. Comparison with geological and seismicity data

We compare present strains results with the deformation rates estimated from seismological and geological data. [37, 38] estimated the rates of horizontal strain and principal axes of the Japanese islands from a 400-year earthquake catalog and the geomorphological data of Quaternary faults. Although the directions of the maximum compressive strains of geological data are in harmony with those obtained from seismological data, the seismic strain release rate is about 30-50% larger than the geological strain rate. Since most of the historical earthquakes are located in the offshore area, where no Quaternary faults are mapped, the geological strain rates may underestimate the strain rate. Therefore, considering the possible unmapped faults, and the uncertainties in the fault slip rates, the difference between the seismic strain rate and the geological strain rate is not significant.

The principal axes estimated in the present study are in agreement with those of seismological and geological data. However, we have a considerable difference in the rates; the present movements are generally one order of magnitude higher than long-term strain rate estimated from seismological and geological data. This difference may be due to aseismic strain resulting from pure folding and/or aseismic slip [37, 39]. Since both the seismic and geological strains rates are small compared with the GPS-derived strain rates, only the aseismic strain due to pure folding would account for part of the difference between the GPS and seismic/geological strain rates. However, Quaternary folding does not seem to be a pervasive feature in Japan [38]. Therefore, this difference should be explained by the non-permanent elastic strain present in the geodetic data transmitted from the subduction zones [37,40]. This interpretation is supported by the results of an elastic dislocation model of the strain field in the Japanese islands [40]. They used a one-year (1995) solution for the velocities of 116 stations of the Japanese arrays to estimate elastic deformation caused by interseismic loading of the Pacific and the Philippine Sea subduction planes. The estimated elastic models account for most of the observed velocity field if the subduction movement of the Pacific plate is 80% locked and if that of the Philippine Sea plate is 100%.

5.2. Crustal stresses and LSPD

Geophysicists have usually assumed that the Japanese islands are purely elastic bodies in the analysis of crustal deformation studies for earthquake prediction. On the other hand, geology and geomorphology studies suggest that the crust deforms not completely elastically especially for long time intervals. To verify this hypothesis, [41] used the inverse method proposed by [42] to study the inelastic properties of the crust in the Japanese islands. He suggested that the Japanese islands deform mostly elastically, and the crustal stresses at surface can well be explained by the simple elasticity theory. Based on this result, the principal axes of stress rates are estimated and shown in fig. 10. In this analysis, Poisson's ratio and rigidity are assumed to be 0.25 and 0.5×10^{11} N/m^2, respectively. Since this pattern is estimated based on the elastic theory, it shows the same characteristics of the principal axes of strain rates fig. 5.

The rate of principal axes of stresses is maximum (8.4×10^{-3} Mpa/yr) in the southern part of the Shikoku district, which may be due to the subducting Philippine Sea plate along the Nankai trough. The larger stresses rate along the coastline near the plate boundary might also indicate that the locking depth of the subducting slab at the Nankai trough is very shallow [43, 30, 44]. In the northern part of the Tohoku district the stresses rate is minimum (2×10^{-3} Mpa/yr) that may be due to the postseismic effect of the 1994 Sanriku [43] earthquake (M7.5).

Fig. 10 also shows a comparison between the directions of the GPS-derived principal axes of stress rates and that of Leading Shear wave Polarization Directions (LSPD) from

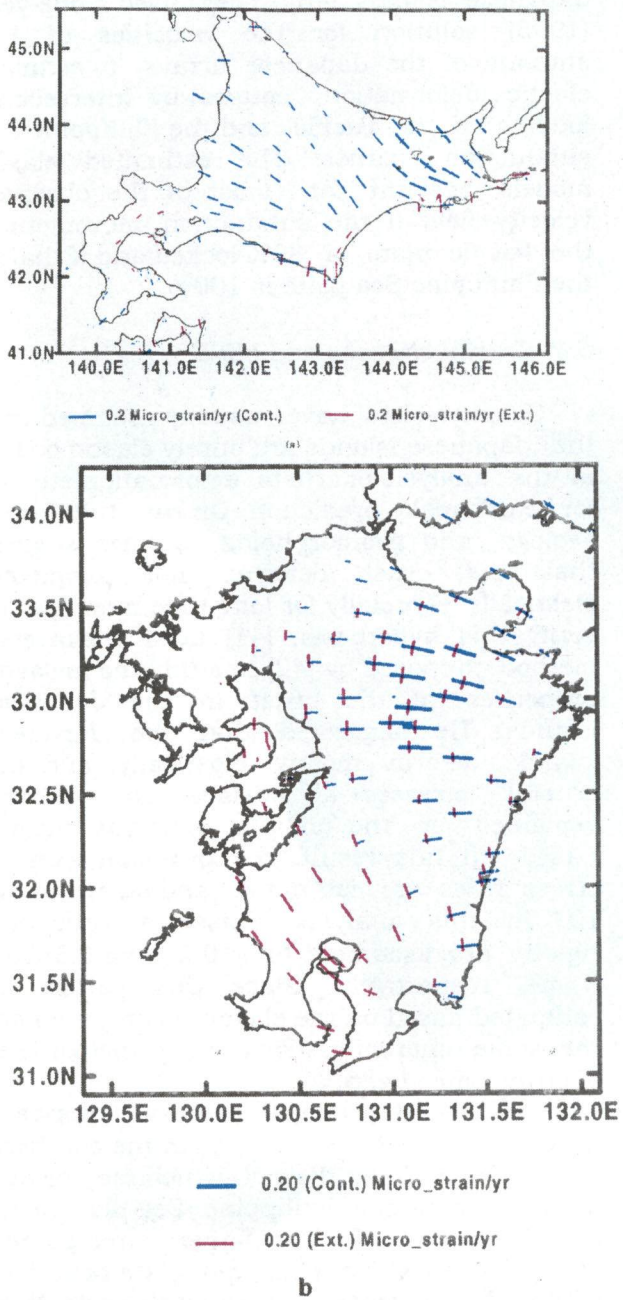

Fig. 9. Magnitude and orientation of principal strains axes in Hokkaido (a) and Kyushu (b) islands as estimated by LSP. The covariance functions shown in Fig. 8 were used.

seismic wave splitting. The LSPD indicates direction of maximum compressional stresses within the crust [45] and if it agrees with maximum compression axes derived from GPS, it implies that the stress orientation by GPS represents that of crustal stress. [46] compiled shear wave polarization data for 10 regions in the Japanese islands. Data of LSPD in fig. 10 was compiled from [46,47]. As it is seen in fig. 10, results of LSPD show a general correlation with GPS stress, suggesting that the stress observed at the surface may represent upper crustal stress, though some exceptional areas such as Shikoku and western part of Kyushu exist.

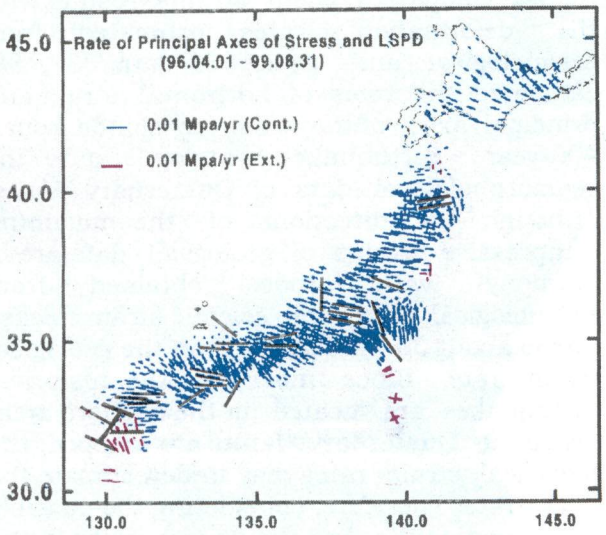

Fig.10. Magnitude and orientation of principal axes of elastic stresses in the Japanese islands estimated based on elastic theory for the period from April 1st, 1996 to August 31st, 1998. The leading shear wave polarization directions (LSPD) (black bars), complied from [46, 47] are also shown.

In Shikoku region, leading shear waves are polarized in the E-W direction at stations in the central area. Whereas the stress rates estimated by GPS has a NW-SE maximum compression, which is somewhat deviated from the shear wave splitting data. On the other hand, leading shear waves in the southern part of the Shikoku island exhibit polarization in the directions of about NEN-SWS, which significantly differs from the direction of GPS stress. The polarization of the stations in the southern part of Shikoku, however, might be doubtful due to an insufficient number of data [47]. In Kaneshima, [47] detected leading shear wave polarizations from crustal earthquakes around a possible rift zone and from upper mantle earthquakes on the Philippine Sea plate. GPS shows N-S extension and E-W compression. Leading shear waves observed at the seismic

stations inside the rift zone show E-W direction, whereas those at the stations located outside or close to the edge of the rift zone fig. 10 are polarized in the N-S direction. In the western part of the area, the Shimabara peninsula, there seems to be significant scatters in the polarization directions of shear waves.

Leading shear wave polarization directions are subject to the pre-existing geological structure and/or reflect the in-situ stress accumulated in the geological time history. On the other hand, direction of maximum compression derived from GPS is instantaneous and will be released by large interplate earthquakes. Although some portion of strains would remain as remnant stress/strain to build up, directions of maximum compression due to LSPD and GPS would naturally be offset.

6. Conclusions

The crustal strains in the Japanese island have been investigated through the LSP technique of GPS data obtained from the dense GPS array for the period of April 1996 to August 1999. Obtained strains seem to portray tectonic environments of the Japanese islands; (1) dilatational strains show that the Japanese islands are under the compressive strain regime induced by the subducting Pacific and Philippine Sea plates, (2) maximum shear strains show a good agreement with recent crustal activities, and (3) principal axes of the strains indicate that the Japanese islands are under the influence from the converging oceanic plates. Although the directions of the maximum compressive strains estimated in the present are in a good agreement with those of seismological and geological data, the GPS strain rates are generally one order of magnitude higher than long-term strains rate estimated from seismological and geological data. This discrepancy might be explained by the non-permanent elastic strain present in the geodetic data transmitted from the subduction zones. On the other hand, the shear stresses at surface of the Japanese islands have been estimated, based on elastic theory. The obtained stresses by GPS observations were compared with the shear wave splitting data that show directions of maximum compression of the upper crust. Results show general agreements with GPS stresses, with some exception.

References

[1] T. Tada, T. Sagiya, S. Miyazaki, The deforming Japanese islands as viewed with GPS, Kagaku (in Japanese) Vol. 67, pp. 917–927 (1997).

[2] S. Miyazaki, T. Saito, M.Sasaki, Y. Hatanaka, and Y. Iimura, Expansion of GSI's nationwide GPS array, Bull. Geogr. Surv. Inst., Vol. 43, pp. 23-34 (1997).

[3] T. Sagiya, S. Miyazaki, and T. Tada, Continuous GPS array and present-day crustal deformation of Japan, Pure appl. Geophys, Vol.157, pp. 2303-2322 (2000).

[4] C. Tsuboi, Investigation on the deformation of the earth crust connected with the Tango Earthquake of 1927. Bull. Earthq. Res. Inst. Vol. 10 (2) (1932).

[5] F. C. Frank, Deduction of earth strains from survey data. Bull. Seism. Soc. America, Vol. 56 (1), pp. 35-42 (1966).

[6] H. M. Bibby, Crustal strain from triangulation in Malborough, New Zealand. Tectonophys, Vol. 29, pp. 529-540 (1975).

[7] T. Rikitake, Earthquake prediction, Elsevier, p. 357 (1976).

[8] J.C. Savage, Strain Patterns and Strain Accumulation Along Plate margins. In application of geodesy to geodynamins, I. Mueller (ed.), Rep. 280, Dept. of Geodetic Sci., Ohio state Univ., pp. 93-97 (1978).

[9] F. K. Brunner, R. Coleman and B. Hirsch, A comparison of computation methods for crustal strains from geodetic measurements. Tectonophys. Vol. 29, pp. 281-298 (1981).

[10] A. Dermanis, Geodetic estimability of crustal deformation parameters. Quatern. Geod, Vol. 2 (2), pp. 159-169 (1981).

[11] p. Benicni A. Dermanis E. Livieratos and D. Rossikopoulos, Crustal deformation at the Friuli area from discrete and continuous geodetic prediction techniques. Annno XLI-bollettino di geodesia e scienze Affini-n. 2 (1982).

[12] A. Dermanis E. Livieratos D. Rossikopulos and D. Vlachos Geodetic

prediction of crustal deformation at the seismic area of Vol. vi, Proc. Intern. Symp. Geodetic Networks and Computations, Munich (1981).

[13] T. Kato, and K. Nakajima, Regional crustal movements in Japan by geodesy and space techniques. J. Geod. Soc. Japan, Vol. 35, pp. 171-185 (1989).

[14] Z. Shen, D. D. Jachson, and B. X. Ge, Crustal deformation across and beyond the Los Angeles Basin from geodetic measurements, J. Geophys. Res., 101, Vol. 27, pp.27. 957- 27.980 (1996).

[15] S. T. Miyazaki, T. Tada, T. Sagiya, D. Sagiya, D. Dong and J. Johnson, Regional crustal deformation of Japan derived by Japanese GPS array, Eos Trans, AGU, Vol. 79, F186 (1998).

[16] K. Heki, Horizontal and vertical crustal movements from three-dimensional very long baseline interferometry kinematic reference frame: Implication for reversal timescale revision. J. Geophys. Res., Vol. 101, pp. 3187-3198 (1996).

[17] H. Moritz, Interpolation and prediction of gravity and their accuracy, Rep 24, Inst. Geod. Phot. Cart. Ohio State Univ., Columbus, USA (1962).

[18] G. S. El-Fiky, T. Kato, and Y. Fujii, Distribution of the vertical crustal movement rates in the Tohoku district, Japan, predicted by least-squares collocation, J. Geodesy, Vol. 71, pp. 432-442 (1997).

[19] G. S. El-Fiky, and T. Kato, Continuous distribution of the horizontal strain in the Tohoku district, Japan, deduced from least square prediction, J. Geodgmaics, Vol. 27, pp. 213-236 (1999a).

[20] H. O. Johnson, and D. C. Agnew, Monument motion and measurements of crustal velocities, Geophys. Res. Lett., Vol. 22, pp. 2905- 2908 (1995)

[21] T. Kato, G. S. El-Fiky, E. N. Oware, and S. Miyazaki, Crustal strains in the Japanese islands as deduced from dense GPS array, Geophys. Res. Lett., Vol. 25, pp. 3445-3448 (1998).

[22] G. S. El-Fiky, Crustal strains in the Eastern Mediterranean and Middle East as derived from GPS observations, Bull. Earthq. Res. Inst., Univ. of Tokyo, Vol. 75, pp. 161-181 (2000a).

[23] K. Nakamura, Possible Nascent trench along the Eastern Japan Sea as the convergent boundary between Eurasian and North American plates, Bull. Earthq. (in Japanese). Res. Inst., Vol. 58, pp. 711-722 (1983).

[24] T. Seno, T. Sakurai, S. Ttein, Can the Okhotsk plate be discriminated from the North American plate? J. Geophys. Res., Vol. 101, pp 27.957-27.980 (1996).

[25] N. Ishikawa, and M. Hashimoto, Average horizontal strain rates in the Japan during interseismic period deduced from geodetic surveys (part 2) (in Japanese), Zishin, Vol. 52, pp. 299-315 (1999).

[26] K. Heki, S. Miyazaki, and H. Tsuji, Silent fault slip following an interplate thrust earthquake at the Japan trench, Nature, Vol. 386, pp. 595-598 (1997).

[27] G. S. El-Fiky, and T. Kato, Interplate coupling in the Tohoku district, Japan, deduced from geodetic data inversion, J. Geophys. Res, Vol. 104, pp. 20361-20377 (1999b).

[28] H. Tsuji, Y. Hatanaka, T. Sagiya and M. Hashimoto, Coseismic crustal deformation from the 1994 Hokkaido-Toho-oki earthquake monitored by a nation wide continuous GPS array in Japan, Geophys. Res. Lett., Vol. 22, pp. 1669-1672 (1995).

[29] T. Sagiya, Boso Peninsula silent earthquake of May 1996, Eos. Trans. 78, F165 (1997).

[30] G. S. El-Fiky, T. Kato, and E. N. Oware, Crustal deformation and interplate coupling in the Shikoku district, Japan, as seen from continuous GPS Observation, J. Tectonophys., Vol. 314, pp. 387-399 (1999).

[31] K. Heki, S. Miyazaki, H. Takahashi, M. Kasahara, F. Kimata, S. Miura, N. vashchenk, A. Ivashchenko, and Ki-Dok An, The Amurian Plate motion and current plate kinematicsin eastern Asia, J. Geophys. Res., Vol. 104 (29), pp. 29.147-29.155 (1999).

[32] T. Tada, Spreading of the Okinawa trough and its relation to the crustal deformation in Kyushu, (in Japanese) Zishin, Vol. 37, pp. 407-415 (1984).

[33] Geographical Survey Institute, Crustal movements in the Kyushu district, Vol. 58, pp. 638-652 (1997).

[34] H. Hirose, K.. Hirahara, F. Kimata, N. Fujii, and S. Miyazaki, A slow thrust slip event following the two 1996 Hyuganada earthquakes beneath the Bungo Channel, southwest Japan, Geophys. Res. Lett., Vol. 26, pp. 3237-3240 (1999).

[35] T. Tabei, T. Ozawa, and Y. Date, Crustal deformation at the Nankai subduction zone, southwest Japan, derived from GPS measurements, Geophy. Res. Lett., Vol. 23, pp. 3059-3062 (1996).

[36] B. Shen-Tu, and W.E. Holt, Interseismic horizontal deformation in northern Honshu and its relationship with the subduction of the Pacific plate in the Japan trench, Geophysical Res. Let., Vol. 23, pp. 3103-3106 (1996).

[37] S. G. Wesnousky, H. Scholz, and K. Shimazaki, Deformation of an island arc: Rates of moment release and crustal shortening in intraplate Japan determined from seismicity and Quaternary fault data, J. Geophys. Res., Vol. 87, pp. 6829-8652 (1982).

[38] B. Shen-Tu, W. E. Holt, and A.J. Haines, Intraplate deformation in the Japanese island: A kinematic study of intraplate deformation at a convergent plate margin, J. Geophys. Res., Vol. 100, pp. 24.275-24.293 (1995).

[39] S. Kaizuka and T. Imaizumi, Horizontal strain rates of the Japanese islands estimated from quaternary fault data. Geogr. Rep. of Tokyo Metropolitan Univ Vol. 19, pp. 43-65 (1984).

[40] X. Le Pichon, S. Mazzotti, F. Henry, and and Hashimoto, Deformation of the Japanese islands and seismic coupling: An interpretation based on GSI permanent GPS observations, Geophys.. J. Int., Vol. 134, pp. 501-514 (1998).

[41] G. S. El-Fiky, Elastic and inelastic strains in the Japanese islands deduced from GPS dense array, EPS, Vol. 52, pp. 1107–1112 (2000b).

[42] M. Hori, T. Kameda, and N. Hosokawa, Formulation of identifying material property distribution based on equivalent inclusion method, J. Struct. Mech. Earthquake Eng., JSCE, pp. 619 I-47 (1999)

[43] T. Sagiya, Crustal deformation Cycle and interplate coupling in Shikoku, Southwest Japan, Ph. D. Thesis, Uinv. of Tokyo, pp. 164 (1995).

[44] T. Ito, S. Yoshioka, S. and Miyazaki, Interplate coupling in southwest Japan Deduced from Inversion Analysis of GPS data, Phys. Of the Earth and Planet. Inter., Vol. 115, pp. 17- 34 (1999).

[45] S. Crampin, A review of wave motion in anisotropic and cracked elastic-media, wave motion, Vol. 3, pp. 343-391 (1981).

[46] S. Kaneshima, Origin of crustal anisotropy: Shear wave splitting studies in Japan, J. Geophys. Res., Vol. 95, pp. 11.121-11.133 (1990).

[47] S. Kaneshima, and M. Ando, An analysis of Split shear wave observed above crustal and uppermost mantle earthquakes beneath Shikoku, Japan: Implications in effective depth extent of seismic anisotropy, J. Geophys. Res., Vol. 94, pp. 14.077-14.092 (1989).

Received September 20, 2001
Accepted December 5, 2001